ISSN : 0974 - 7486 Volume 9 Issue 1

Trade Science Inc.

Materials Science

An Indian Journal

Full Paper

MSAIJ, 9(1), 2013 [36-40]

# Synthesis, characterization and ionic conductivity of oxyphospho-silicates with apatite structure

**Mohamed Abbassi[1], Riadh Ternane[1]*, Adel Madani[2], Malika Trabelsi-Ayadi[2]**

[1]Laboratoire d'Application de la Chimie aux Ressources et Substances Naturelles et à l'Environnement, Université de Carthage, Faculté des Sciences de Bizerte, 7021 Zarzouna Bizerte, (TUNISIA)

[2]Laboratoire de Physique des Matériaux, Université de Carthage, Faculté des Sciences de Bizerte, 7021 Zarzouna Bizerte, (TUNISIA)

E-mail: rternane@yahoo.fr

*Received: 28th April, 2012; Accepted: 9th October, 2012*

## ABSTRACT

Oxyphospho-silicates with apatite structure $Ca_{2+x}La_{8-x}(SiO_4)_{6-x}(PO_4)_xO_2$ were synthesized by solid state reaction at high temperature. The obtained materials were characterized by powder X-ray diffraction, infrared absorption spectroscopy and Raman scattering spectroscopy. Electrical properties of the materials have been studied by the complex impedance spectroscopy. The electrical conductivity measured in a wide range of temperature increases with silicon content. For each composition, the ionic conductivity obeys the Arrhenius law. A mechanism of the oxide ion conduction is proposed. 

## KEYWORDS

Apatites;
Oxyphospho-silicates;
Complex impedance spectroscopy;
SOFC.

## INTRODUCTION

Apatites are solid inorganic compounds, represented by the general formula $Me_{10}(XO_4)_6A_2$, they crystallize in the hexagonal system with the space group $P6_3/m$[1]. The apatite structure provides a great capacity to form solid solutions and, particularly, to accept several substitutes for example, the monovalent A ion can be $OH^-$, $F^-$, $O^{2-}$, $CO_3^{2-}$…, the trivalent anion $XO_4$ can be $AsO_4^{3-}$, $VO_4^{3-}$, $CrO_4^{3-}$, $HPO_4^{2-}$, $CO_3^{2-}$, $SiO_4^{4-}$, $SiO_3N^{5-}$. There is no literature information showing that vacancies could exist on this site. Me cations may be bivalent, or monovalent or trivalent ($Ba^{2+}$, $Pb^{2+}$, $K^+$, $La^{3+}$). The apatite-like structure is characterized by the presence of two types of tunnels permitting the location of two cationic sites labeled Me (I) and Me (II): four Me (I) are at the centre of narrow tunnels (4f sites), six Me (II) around large tunnels (6h sites) the centers of which are occupied by $A^-$ anions located on the hexad axis (2a sites). The coordination number of Me (I) site is nine, whereas for Me (II), it is seven.

Because of the mobility of Me and A ions in such compounds, investigations on electrical properties were performed. Several authors have established a correlation between structural properties and ionic conductivity[2-4]. Apatite materials have attracted considerable interest for a range of applications, including electrolytes for solid oxide fuel cells (SOFC). Their electrical properties were largely studied. Recently, it was found that some apatite-type rare earth silicates can exhibit high oxide-ion conductivity[5-11].

## EXPERIMENTAL PROCEDURE

Apatite powders $Ca_{2+x}La_{8-x}(SiO_4)_{6-x}(PO_4)_xO_2$ have been synthesized by high temperature solid state reaction using starting materials $SiO_2$, $CaCO_3$, $(NH_4)_2HPO_4$ and $La_2O_3$ with defined proportions. The mixture was primarily heated up to 1173 K for 24h and calcinated at 1673 K for 6 h, according to the following reaction:

**$(2+x)\ CaCO_3 + 4-(x/2)\ La_2O_3 + (6-x)\ SiO_2 + x\ (NH_4)_2HPO_4 \rightarrow Ca_{2+x}La_{8-x}(SiO_4)_{6-x}(PO_4)_xO_2 + 2x\ NH_3 + (2+x)\ CO_2 + 3x/2\ H_2O$**

The X-ray diffraction were carried out by a BRUKER D8-advance diffractometer using Cu Kα radiation (λ = 1.5406 ú). Cell parameters were refined with the «celref» program. The Infrared (IR) spectra were recorded on a Bruker spectrometer, in the 4000–400 $cm^{-1}$ range, using the KBr pellet technique.

The Raman spectra were recorded using a DILOR XY spectrometer equipped with a CCD detector and a spectra physics Ar laser (excitation at 514.5 nm).

For electrical properties, impedance spectroscopy measurements have been performed after both sides of the sintered disc were coated with Ag paste. The measurements have been made in the frequency range 5Hz–13 MHz at different temperatures. The apparatus used is a Hewlett-Packard 4192A analyzer of impedance.

## RESULTS AND DISCUSSION

### Characterization

### X-ray powder diffraction

The X-ray diffraction patterns show that $Ca_{2+x}La_{8-x}(SiO_4)_{6-x}(PO_4)_xO_2$ apatites crystallize in the hexagonal system with the space group $P6_3/m$.

The variations of the a and c parameters are given in Figure 1, The decrease of a and c parameters are attributed to the substitution of $SiO_4^{4-}$ and $La^{3+}$ ions by smaller $PO_4^{3-}$ and $Ca^{2+}$ ions ($Si^{4+}$ (0.355 Å), $La^{3+}$ (1.032 Å), $P^{5+}$ (0.17 Å), $Ca^{2+}$ (1.00 Å))[12]. Moreover, the continuous evolutions of a and c unit cell parameters follow the Vegard's law. This indicates the occurrence of a continuous solid solution inside the defined single-phase domain of oxyphospho-silicates.

Changes in peak position and intensity are observed because of the change in concentration of $PO_4^{3-}$ and

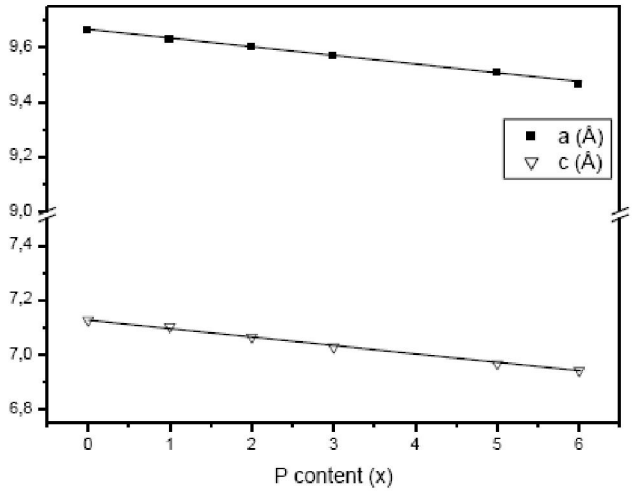


**Figure 1 : Variation of a and c unit-cell parameters of $Ca_{2+x}La_{8-x}(SiO_4)_{6-x}(PO_4)_xO_2$ oxyapatites versus P content**

**TABLE 1 : Lattice parameters and crystallite size of $Ca_{2+x}La_{8-x}(SiO_4)_{6-x}(PO_4)_xO_2$ oxyapatites**

| x [P content] | a (Å) | c (Å) | d (nm) | Lattice strain (%) |
|---|---|---|---|---|
| 0 | 9.661 | 7.126 | 2.855 | 5.735 |
| 1 | 9.630 | 7.102 | 2.844 | 5.772 |
| 2 | 9.602 | 7.063 | 2.850 | 5.735 |
| 3 | 9.570 | 7.027 | 2.850 | 5.846 |
| 5 | 9.507 | 6.966 | 2.842 | 5.806 |
| 6 | 9.465 | 6. 941 | 2.833 | 5.781 |

$Ca^{2+}$. By using some reflections of XRD pattern (widely scattered in 2r), the coherently scattered crystallite size and lattice strain of the samples was calculated from the X'Pert HighScore software using Scherrer's calculator ($d_{hkl} = d = \frac{0.9\lambda}{\beta\cos\theta}$); where d is the average crystallite size, λ is the wavelength of Cu-Kα radiation, β is the full width at half maximum of the diffraction peak and r is the Bragg diffraction angle. All the parameters are given in TABLE 1.

### Vibrational infrared and Raman spectra

Because of the similarity between the tetrahedral groups $SiO_4^{4-}$ and $PO_4^{3-}$, it is difficult to assign their bands. Band assignment was carried out from the studies related to the various vibration modes of the different apatites[13-16].

The infrared and Raman spectra of the $Ca_{2+x}La_{8-x}(SiO_4)_{6-x}(PO_4)_xO_2$ oxyapatites are given in Figure 2 and Figure 3, respectively. Some interesting remarks have to be noted:

- The bands attributed to stretching and libration modes of $OH^-$ ions at 3572 $cm^{1-}$ and 630 $cm^{-1}$,

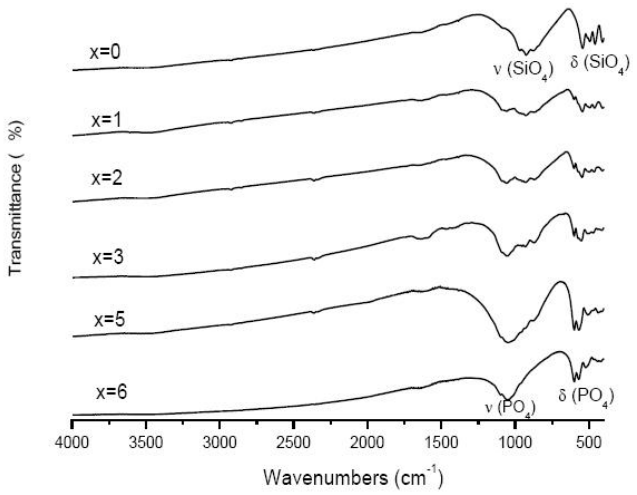


**Figure 2 : IR spectra of $Ca_{2+x}La_{8-x}(SiO_4)_{6-x}(PO_4)_xO_2$ oxyapatites**

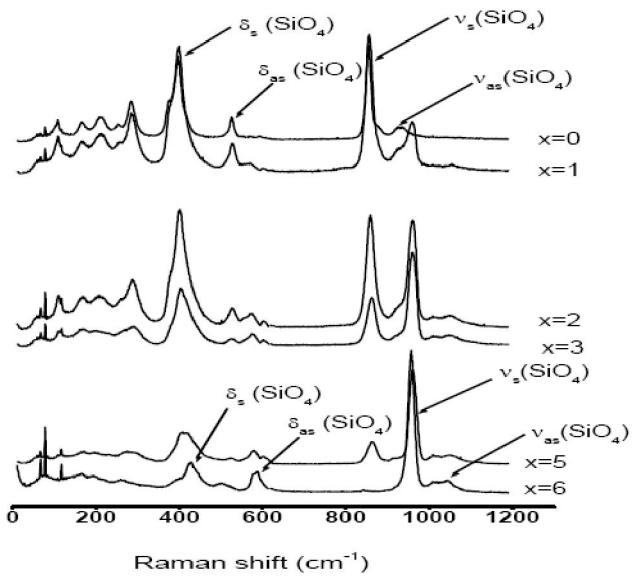


**Figure 3 : Raman spectra of $Ca_{2+x}La_{8-x}(SiO_4)_{6-x}(PO_4)_xO_2$ oxyapatites**

respectively, were not detected, it proves that the prepared samples do not contain hydroxyls ions.

- The absence of the band at 850 $cm^{-1}$, attributed to peroxide ion ($O_2^{2-}$)[17].
- Both IR and Raman spectra continuously vary with the substitution of $SiO_4^{4-}$ ions by $PO_4^{3-}$ ions.

When all the silicate groups were replaced by phosphate groups, the IR spectrum exhibits a broad band between 1200 and 800 $cm^{-1}$ formed by the vibrational bands $\nu_{as}$ (920 and 967$cm^{-1}$) and $\nu_s$ (870 $cm^{-1}$) of $SiO_4^{4-}$ ions.

At lower frequencies, five bands were assigned to $\delta_{as}$ modes (493, 542, and a shoulder at 512 $cm^{-1}$) and $\delta_s$ modes (404 and 456 $cm^{-1}$) of silicate groups. In this frequency range, the $\delta_{as}$ modes of $PO_4^{3-}$ anions progressively appear with increasing $PO_4$ content whereas the two bands at 456 and 493 $cm^{-1}$ shift towards higher frequency and finally the broad band at 419 $cm^{-1}$ of $PO_4$ appears.

In the IR and Raman spectra, the relative intensity attributed of the bands assigned to $PO_4$ and $SiO_4$ groups agrees with the change of $PO_4/SiO_4$ ratio.

## Electrical properties

A typical example of complex impedance plot is shown in Figure 4 for the *$Ca_2La_8(SiO_4)_6O_2$ oxyapatite.*

The bulk response is associated with the semi-circle at high frequencies centered on the axis representing

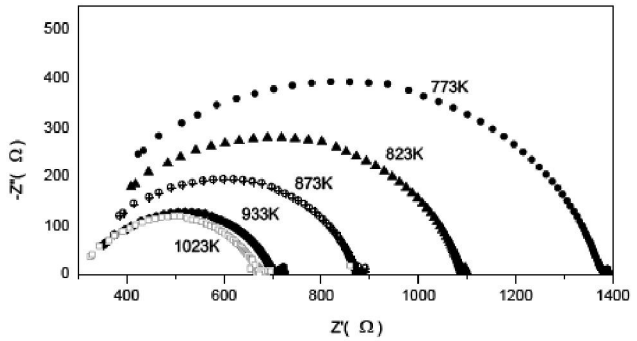


**Figuer 4 : Complex impedance spectra of $Ca_2La_8(SiO_4)_6O_2$ oxyapatite at different temperatures**

the real parts of the impedance. Impedance spectra were fitted satisfactorily with a parallel R-CPE circuit model and R was extracted.

The bulk components were considered in order to determine the conductivity values noted σ. These values are calculated with the formula σ = –!/RS (R is the resistance obtained from impedance diagrams by intercepting impedance spectra with real axis, *S* and –! are the area and the thickness of the sample, respectively).

The temperature dependence of bulk conductivities is represented in Figure 5. A linear variation is observed in Arrhenius plots, following the relation:

$$\sigma = \frac{A}{T}\exp(-\frac{Ea}{kT})$$

Where $E_a$ is the activation energy, k is the Boltzmann constant and A is pre-exponential factor.

Activation energy has been calculated from the linear fitting of the conductivity data.

TABLE 2 gives activation energy of electrical bulk conductivity for different compositions.

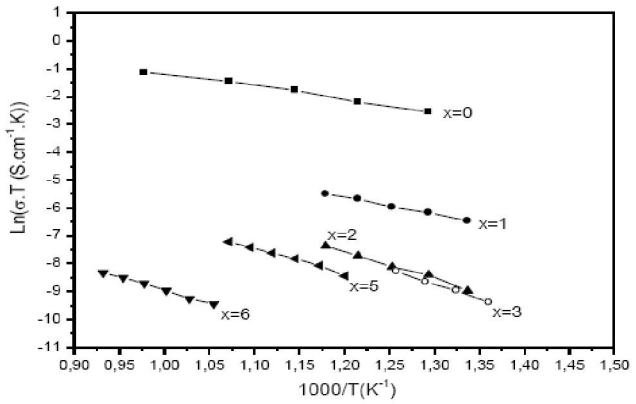


**Figure 5 : Arrhenius plot Ln (σT) = f (1000/T) of ionic conductivity of $Ca_{2+x}La_{8-x}(SiO_4)_{6-x}(PO_4)_xO_2$ oxyapatites**

The pure silicate oxyapatite is found to be better conductor than the other materials.

An increase of the activation energy value is observed with Ca and $PO_4$ substitutions. The variation of the activation energy can be explained by the mobility of the $O^{2-}$ ions in the large tunnels formed by Me (II) cations and the variation of the electrostatic interactions between $O^{2-}$ ions and X of $XO_4$ tetrahedrons (X=P, Si).

**TABLE 2 : Activation energy of $Ca_{2+x}La_{8-x}(SiO_4)_{6-x}(PO_4)_xO_2$ oxyapatites**

| x [P content] | Activation energy $E_a$ (eV) |
|---|---|
| 0 | 0.392 |
| 1 | 0.528 |
| 2 | 0.854 |
| 3 | 0.771 |
| 5 | 0.91 |
| 6 | 0.794 |

The conductivity in these materials follows the relationship:

$$\sigma = n \mu q$$

Where σ, n, μ and q design the conductivity, the charge density, the mobility and the charge value, respectively.

In this expression, the mobility is the dominant factor in the conductivity of these apatites. The apatite tunnels formed by $SiO_4^{4-}$ ions are wider than that by $PO_4^{3-}$ ions; this fact provides a better mobility of $O^{2-}$ ions along the framework. On the other hand, the free $O^{2-}$ ions are weakly attracted by less electronegative $Si^{4+}$ than by $P^{5+}$.

## CONCLUSION

This paper presents a study of synthesis, characterization and ionic conductivity of $Ca_{2+x}La_{8-x}(SiO_4)_{6-x}(PO_4)_xO_2$ oxyapatites. X-ray diffraction study shows that these materials crystallize in the hexagonal system with $P6_3/m$ as space group. Infrared and Raman spectra are reported and band assignments are made.

The temperature dependence of the electrical conductivity follows an Arrhenius type law with temperature.

It was highlighted an increase of the ionic conductivity with a decrease of in the activation energy, as the phosphate content decreases. This increase is related to the variation of volume of the cell and displacement of $O^{2-}$ ions in large tunnels of apatites.

## ACKNOWLEDGEMENTS

The authors would like to thank Gerard PANCZER, Professor at the University Claude Bernard Lyon I, for his invaluable assistance in the realization of the Raman spectra.

## REFERENCES

[1] J.S.Prener; J.Solid State Chem., **3**, 49 **(1971)**.
[2] M.Mehnaoui, R.Ternane, A.Madani, M.Trabelsi-Ayadi; J.Phys.IV, **122**, 135 **(2004)**.
[3] E.Chakroun, R.Ternane, D.Ben Hassen-Chehimi, M.Trabelsi-Ayadi; Mat.Res.Bull., **43**, 2451 **(2008)**.
[4] A.Orera, D.Headspith, D.C.Apperley, M.G. Francesconi, P.R.Slater; J.Solid State Chem., **182**, 3294 **(2009)**.
[5] J.E.H.Sansom, D.Richings, P.R.Slater; Solid State Ionics, **139**, 205 **(2001)**.
[6] J.E.H.Sansom, E.Kendrick, J.R.Tolchard, M.S Islam, P.R.Slater; J.Solid State Electrochem., **10**, 562 **(2006)**.
[7] A.Vincent, S.Beaud, Savignant, F.Gervais; J.Eur.Ceram.Soc., **27**, 1187 **(2007)**.
[8] E.Kendrick, M.S.Islam, P.R.Slater; Solid State Ionics, **177**, 3411 **(2007)**.
[9] S.Chefi, A.Madani, H.Boussetta, C.Roux, A.Hammou; J.Power Sources, **177**, 464 **(2008)**.
[10] P.J.Panteix, V.Baco-Carles, Ph.Tailhades, M. Rieu, P.Lenormand, F.Ansart, M.L.Fontaine; Solid State Sciences, **11**, 444 **(2009)**.
[11] B.Li, W.Liu, W.Pan; J.Power Sources, **195**, 2196 **(2010)**.
[12] R.D.Shannon; Acta.Cryst., **32**, 751 **(1979)**.

**[13]** S.Khorari, R.Cahay, A.Rulmont, P.Tarte; J.Solid State Inorg.Chem., **31**, 92 **(1994)**.
**[14]** J.Neubauer, H.Pollmann; N.Jb.Miner.Abh., **168**, 237 **(1995)**.
**[15]** R.Ternane, M.Th.Cohen-Adad, G.Panczer, C.Goutaudier, N.Kbir- Ariguib, M.Trabelsi-Ayedi, P.Florian, D.Massiot; J.Alloys Compd., **333**, 62 **(2002)**.
**[16]** R.El Ouenzerfi, C.Goutaudier, G.Panczer, B.Moine, M.T.Cohen-Adad, M.Trabelsi-Ayedi, N.Kbir-Ariguib; Solid State Ionics, **156**, 209 **(2003)**.
**[17]** J.C.Trombe; Ann.Chim.Fr., **8**, 335 **(1973)**.